Chapter

Ionospheric Scintillation Modeling Needs and Tricks

Shishir Priyadarshi

Abstract

The wavelength of the radio-wave satellite signal is of the order of the minimal small-scale ionospheric irregularities (i.e., a few centimeters). As the satellite signal passes through the ionosphere, its interaction with the ionospheric irregularity structures causes refraction, reflection, and polarization in the satellite signal. Ionospheric irregularities degrade the trans-ionospheric radio-wave signal quality, between the satellite and the receivers, due to scintillation. The physics-based model often fails to produce global morphology during the extreme solar events, whereas empirical models based on the ionospheric scintillation data demonstrate better quality to forecast the scintillation effects during extreme solar event. It is really tricky to make a scintillation model that is sensitive to low and high solar activities as well as extreme solar events simultaneously. In the presented book chapter, we will discuss/review the needs and tricks of modeling ionospheric scintillation during extreme solar events as well as all weather and latitudinal cases. There are several aspects that influence the scintillation occurrence, its strength, and global distribution. The latitudinal dependence, local weather, solar/geomagnetic activity conditions, and local times are the widely accepted factors that control and influence ionospheric scintillation most. This book chapter discusses all these aspects and also suggests the ways to cast aside those factors that led to the wrong measure of scintillation indices.

Keywords: ionospheric scintillation, empirical scintillation model, GPS/GNSS scintillation modeling, global scintillation model

1. Introduction

Whenever the radio-wave signals pass through the ionospheric irregularities, these signals feel reflection, refraction, and scintillations (i.e., sharp and rapid carrier-phase variations and signal-to-noise ratio fading). In general it is more typical when the carrier-phase loss of lock happens due to the sharp signal-to-noise ratio fading ([1, 2] and references therein). As the wave propagates to the ground, scintillation models are needed to produce global as well as local ionospheric scintillation data and maps during the required solar activity condition, day, season, and geographic locations. Generally, scintillation models are made to serve special needs and not for all the spatial and temporal situations; due to this generally each scintillation model is not fit for all the geographic and solar activity conditions.

In general, scintillation models often have two significant limitations; firstly physics-based models often fail in producing scintillation morphology during

extreme solar and geomagnetic events. The second limitation is there is no possibility of a correction in the model once its algorithm is derived. In the presented book chapter, scintillation empirical modeling methods and their limitations are discussed. Geometrical effects contaminate scintillation observations most. We have discussed in this chapter how to overcome scintillation modeling limitations and use some tricks that replicate the actual scintillation morphology. The presented text in this chapter will enrich the knowledge of ionospheric modelers and make them understand how beginners should proceed with the ionospheric scintillation or ionospheric electron density as a model input data, if they decided to model certain ionospheric parameters (such as spectral index, turbulence strength parameters of the ionospheric irregularities, amplitude and phase fluctuations, scintillation indices, etc.).

2. Scintillation modeling tricks and correction for the geometry of propagation

As the elevation angle of the signal wave source changes, we observe the changes in the intensity of ionospheric scintillation. Such changes are significant as they are caused due to enhancement in the path of the radio-wave signal through the ionospheric irregularity layer with decreasing elevation angle and vice versa [3]. The signal ray path through the ionospheric irregularity also depends on the size and orientation of the ionospheric irregularity structure along with the height and thickness of the ionospheric irregularity layer [1]. All these elements influence the intensity of the ionospheric scintillation, and the effect caused by them on the trans-ionospheric radio-wave is termed as the geometrical effect [3–5]. In this section, we will cover the scintillation modeling tricks and method to minimize the multipath effect and impact ways to overcome other geometrical effects such as irregularity orientation with respect to the local geomagnetic field lines, multipath at higher elevation angle, radio-wave signals' extended path near the Earth's horizon, etc.

2.1 Scintillation modeling tricks

For the empirical scintillation modeling, first, we should need to have data for all the seasons and solar as well as geomagnetic activity situation. For instance, if we are planning to model ionospheric scintillation during high solar activity in winter months, we must have winter-month data collected during high solar activity period. Similarly, for the low solar activity period and in particular month scintillation modeling, we must have alike data. An adequate empirical modeling study expands understanding of ionospheric irregularities and can be used to better evaluate the impact of scintillation on different resources. The physics-based model often fails to produce global morphology during extreme solar events, whereas empirical models based on the ionospheric scintillation data demonstrate better scintillation effects during extreme solar events. It is really tricky to make a scintillation model which is sensitive to low and high solar activities as well as extreme solar events simultaneously.

The modeler should also derive the relationship between solar activity and provisional activity indices with the ionospheric scintillation data in order to make the scintillation data sensitive to the solar activity condition. One should always keep in mind that all the solar activity, geomagnetic, and provisional indices are not equally beneficial to all the geographic locations. Therefore, one should use the proper geo, solar, and provisional activity indices for specific geographic locations. If the modeler is planning to develop a global ionospheric scintillation model, they

should always keep in mind that their algorithm should be sensitive to the geographic locations, solar activity as well as local weather. This can be achieved by having different derivation algorithm for each and every geographic location, and the final algorithm should combine all these sub-algorithm to demonstrate the global scintillation response.

2.2 Geometrical error correction and lower elevation multipath

It is better to have the latest data for modeling new events, but, in case of new data unavailability, the previous data may be from the previous solar cycle [6]. The latest data are generally close to the new solar/or geomagnetic event, and they are from the same solar cycle activity period. Therefore, the scintillation models based on the latest data are comparatively closer to the new observations in comparison to the data from the previous solar cycles. The advent of scintillation effect on the trans-ionospheric radio-wave signal lower elevation angles ($\leq 20°$) is being discarded from the data to minimize the effect of multipath. Multipath can occur on any elevation angle. To reduce the high-elevation angle, multipath scintillation receiver's antenna must be setup to minimize CODE and PHASE reflections (multipath), by mounting it away from close reflecting surfaces [6]. The multipath effect also depends on the PRN code rate (please see [7] for details). Moreover the multipath effect can appear at higher elevation angles than 20° (please see [8] for details). Multipath effects occurring at any elevation can be minimized by the geometrical corrections in the data [2]. But, to do it one should be well familiar with the other high-altitude structures (such as mountains or high-altitude building, etc.) near the GPS/GNSS receivers' location and filter the datasets reflected from such structures to reduce the multipath effect. To avoid the high-altitude structures, we have to manual check the data and avoid those elevation angles which show unusual enhancement in the scintillation indices. Following Rino [9], ionospheric irregularities orient themselves according to the local geomagnetic field lines. The phase lock loss highly depends on the angle between the geomagnetic field lines and receiver-transmitter line of sight [10, 11]. For example, at the polar ionosphere, ionospheric irregularities often form rodlike structure and orient themselves along the vertical geomagnetic field lines, whereas at the mid and equatorial latitudes, the local geomagnetic field line is merely horizontal to the Earth's surface due to which sheet- or winglike ionospheric irregularity structures frequently appear. If the irregularity orientations are along the geomagnetic field lines, they form a rodlike structure; if the ionospheric irregularity orientation is across the geomagnetic field lines, it may appear either as a wing- or as a sheetlike structure. We are addressing both cases (rodlike structure and the high-latitude and sheet-/winglike structure at the equatorial and mid-latitude) in this book chapter.

Following Rino [9] and Booker [12], phase and amplitude scintillations can be expressed as follows:

$$<\delta\varphi^2> = r_e^2\lambda^2(Lsec\theta)GC_s\frac{q_0^{-2\vartheta+1}\Gamma\left(\upsilon-\frac{1}{2}\right)}{4\pi\Gamma\left(\upsilon+\frac{1}{2}\right)}F(a,b) \tag{1}$$

$$S_4^2 = r_e^2\lambda^2(Lsec\theta)C_sZ^{\upsilon-1/2}\frac{\Gamma\left(\frac{2.5-\upsilon}{2}\right)}{2\sqrt{\pi}\Gamma((\upsilon+0.5)/2)(\upsilon-0.5)}\mathcal{G}\,F(a,b) \tag{2}$$

where r_e is the classical electron radius; λ is the wavelength of the signal; L is the irregularity slab thickness; θ is the satellite zenith angle; C_s is the turbulence strength parameter, which is a function of the fluctuation in the electron density ($\Delta N/N$) in the irregularity slab along the satellite signal path; G is the geometric

S. No.	Elongation parameters' axial ratio	Ionospheric irregularity form
1	a:1 (i.e., b = 1)	Field aligned rods
2	a:a (i.e., a = b)	Sheets elongated both along the magnetic field and in transverse plane coinciding with local L shell
3	a:b and a > b	Like wings
4	a:b and a < b	This combination is impossible, as ionospheric structures cannot have their spread more in transverse direction of the geomagnetic field

Table 1.
Form of the ionospheric irregularities.

factor and is a function of ionospheric irregularity elongation parameters F(a,b), "a" is the elongation parameter of the irregularities along the filed lines and "b" is used for elongation across the geomagnetic field lines; υ is the three-dimensional spectral index; q_0 is the inner scale constant and $Z \rightarrow \frac{\lambda Z_R Sec\theta}{4\pi}$; $Z_R = ZZs/(Z + Z_s)$ and Z_s are the distance to the source; $\mathcal{G}$ is the common geometry and propagation factor, which is also a function of elongation parameters a and b; and $<\delta\varphi^2>$ is the phase variance in the satellite signal after passing through the ionospheric irregularity.

Following the assumption of the theory of wave propagation in random medium, it is safe to assume at the signal frequency of interest that only the phase of the signal wave gets distorted [2] as the signal passes through the ionospheric irregularity of slab thickness L, and GPS scintillation receivers can observe the time series of the phase-modulated signal on the ground. Formulas (1) and (2) can be used to simulate the amplitude and phase scintillation. Study of the power spectrum of the ionospheric data improves the estimation of the local ionospheric irregularity form and their orientation with respect to the local geomagnetic field. Several ionospheric parameters such us spectral index, turbulence strength parameter, and phase fluctuations are essential for correcting the data contaminated through the geometrical errors.

Following Eq. (2) discussed in Rino [9], scintillation index is a function of Fresnel filter factor F(a,b) which is a function of elongation parameters "a" and "b." A detailed explanation of this function is discussed in Rino [9]; as it is beyond the scope of this book chapter therefore we are not discussing it in more details. But, for the reader's convenience, we are providing a summary table (please see **Table 1**), which summarizes the different combinations of "a" and "b" giving rise to different ionospheric irregularity shapes.

3. Scintillation modeling needs and discussions

Scintillation modeling provides a general scenario of the ionospheric scintillations' global morphology and occurrence during different solar activity and space weather conditions. It is always not possible to obtain ionospheric scintillation observation during some space weather events, and during such situations, a realistic ionospheric scintillation model can be used to fill the data gaps. On the other hand, data assimilation techniques also use scintillation model to assimilate scintillation observation into the scintillation model in order to improve the forecast.

There are two aspects that influence the occurrence and strength of the ionospheric scintillation. First is the geometrical effect between the radio-wave-emitting satellite and the receiver which can be at any different location, e.g., at the ground;

on a moving object such as vehicles, ships, or airplanes; onboard at any beacon satellites; or on a spacecraft. The geometrical effect is highly dependent on the elevation angle at which the receiver receives the satellite signal, azimuth angle of the receiver, and orientation of the ionospheric irregularity structures with respect to the local geomagnetic field. The geometrical effects also depend on the angle between the signal ray path and the local geomagnetic field. Another important aspect that influences the scintillation morphology and the rate is the combination of several things such as the geographic location of our region of interest, local season, local time, solar activity condition, during a geomagnetic quite day or a geomagnetically disturbed day, etc. Here first we will discuss in details the geometrical influence on the ionospheric scintillation using the illustrative examples and demonstrate the influence of the geometrical correction on the satellite signal.

3.1 Influence of the geometrical effects over the scintillation estimation and the way to remove these errors

In Eq. (1) the height of the ionospheric irregularity from the Earth's surface Z is a function of sec(θ). The zenith angle (θ) is a function of elevation angle (E) and can be expressed as

$$\theta = 90 - E \tag{3}$$

Using the relation between satellite and zenith angle, Eq. (2) can be simplified as

$$S_4 \sim \left[\sec\ (90 - E)\ \sec\ (90 - E)^{\upsilon - 1/2}\right]^{1/2} \tag{4}$$

As we mentioned earlier, υ is a three-dimensional ionospheric irregularity spectral index [9]. One-dimensional spectral index (p) is related to the three-dimensional spectral index as p = 2υ−1. If we simplify Eqs. (3) and (4), we will get to a direct dependence relationship between scintillation indices and zenith angle. Following Priyadarshi and Wernik [13], we can derive the spectral index p by using the log-log relationship of the scintillation index observation and cosecant of the satellite elevation angle [13]:

$$S_4 \sim \csc(E)^{(p+2)/4}\ F(a, b) \tag{5}$$

From Eq. (5) it is clear that the scintillation index is a power-law function of cosecant of the elevation angle with the power one-dimensional ionospheric irregularity spectral index (p) [13]. In order to simplify it more and avoid the dependence on the filter factor F(a,b), which is a complicated function of the ionospheric irregularity elongation parameters and which makes the overall ionospheric irregularity orientation dependence very complicated [13], we have considered the ionospheric radio-wave propagation environment as isotropic [9], and this turns F(a, b) = 1. Now if we plot log-log maps for S_4 and Sin (E) angle, we can calculate the one-dimensional spectra index (p) from this relationship. Once we have spectral index, we can correct the scintillation for the geometry of propagation between the receiver and the transmitter using the Eq. (6):

$$S_{4\_corrected} = S_{4\_observed}/\csc(E)^{(P+2)/4} \tag{6}$$

Figure 1 shows the non-corrected ($S_{4\_observed}$) Vs-corrected scintillation indices ($S_{4\_corrected}$) observed from the GPS scintillation receiver GSV 4004b deployed at

the Hornsund, Svalbard (76.9718° N, 15.7844° E). The red dots show the amplitude scintillation index, whereas the black dots show the phase scintillation index. If we compare these two figures, the gap between amplitude and phase scintillation index is very less in uncorrected case (on the left). We see that the number of amplitude and phase scintillation observations is reduced in the corrected case (on the right). It is evident from **Figure 1** that after correcting the scintillation data, we come over the geometrical effect for the amplitude as well as phase scintillation. After the geometrical effect correction, we observe two main things. Firstly, there is a reduction in the numerical peak value of the scintillation indices, and secondly, we do see the significant numerical level gap between amplitude and phase scintillation index data after the geometrical correction.

Figure 2 shows the normalized simulated scintillation index map (scintillation index divided by the scintillation index at 25° elevation angle). This map shows the scintillation index simulation for a high-latitude station in Hornsund, Svalbard.

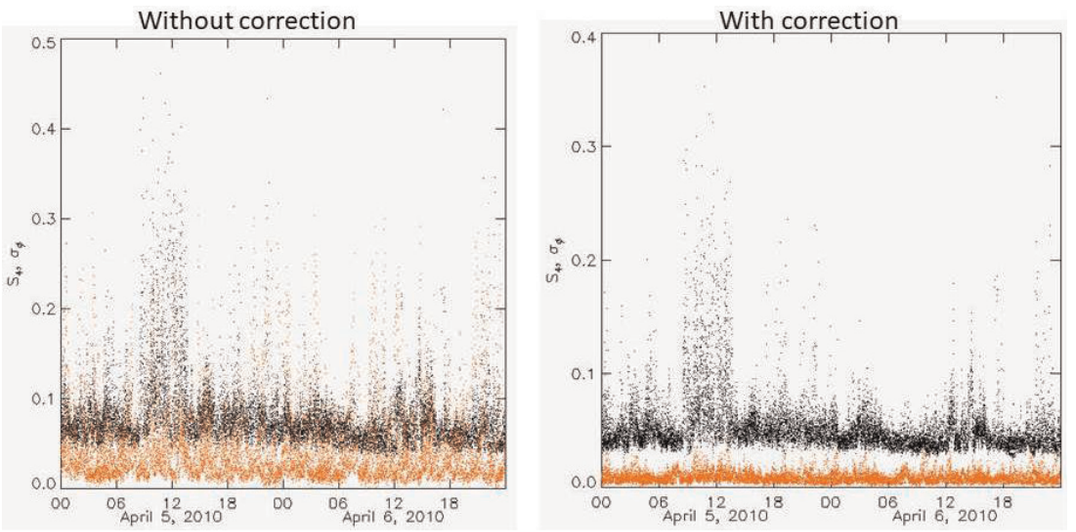

Figure 1.
Amplitude (in orange) and phase scintillation (in black) index observations for Hornsund, Svalbard (76.9718° N, 15.7844° E), (on left) without geometrical effect correction, (on right) with geometrical effect correction.

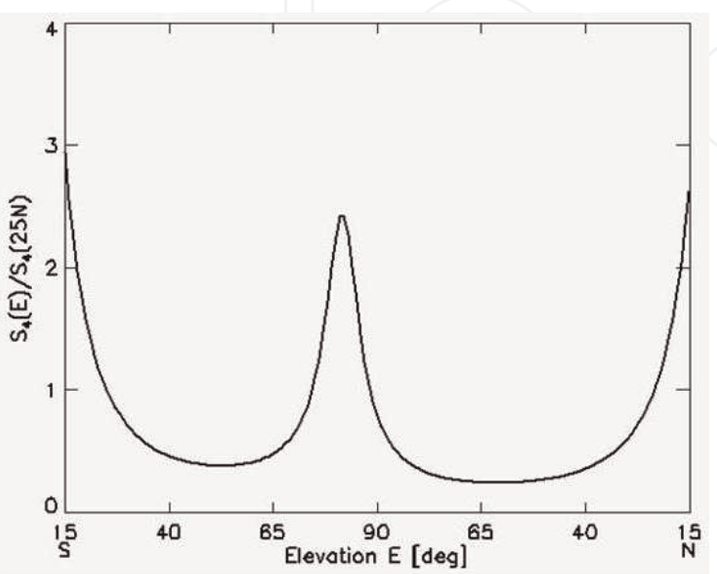

Figure 2.
Normalized simulated amplitude scintillation index for Hornsund, Svalbard, vs elevation angle of the transmitter.

Here we see the scintillation index maximizes between 15 and 20° elevation angles as well as between 70 and 85° elevation angles. At 15–20° elevation angle, the multipath effects are dominant due to which we observe high-value scintillations. On the other hand, between 70 and 85° elevation, the angle orientation of the geomagnetic field line at Hornsund is such that it forms rodlike structure along the geomagnetic field lines. At certain combination of the elevation and azimuth angle, the receiver looks along the geomagnetic field lines. Due to such ionospheric irregularity structure orientation, GPS/GNSS signal travels more distance through the ionospheric irregularity; consequently, we observe the high numerical value of the scintillation indices at this elevation angle range.

To demonstrate the simultaneous impact of the ionospheric irregularity structure and its orientation with respect to the local geomagnetic field lines, we have simulated amplitude scintillation index for a mid-latitude regions Weihai (geographic latitude 37.53°, geographic longitude 122.05°). We have simulated a mid-latitude region for simulating the scintillation index (please see **Figure 3**) using the method discussed in Priyadarshi and Wernik [13] because at the mid-latitude orientation of the geomagnetic field line is neither completely horizontal (alike the equatorial region) nor completely vertical (as at the polar region).

Such slant orientation of the geomagnetic field with respect to the local Earth's surface allows the ionospheric irregularities to evolve and settle in several forms. The orientation parameters along and across the geomagnetic field lines are shown in **Figure 3a** and **b**. The top-left panel shows the rodlike structure, in which we see that for lower elevation angle (≤10°), the scintillation index is very high. As the elevation angle gradually increases, there is a reduction in the scintillation index, and the scintillation index is minimal for higher elevation angle (≥70°). It means that when the spread of the ionospheric irregularity is not significant neither along

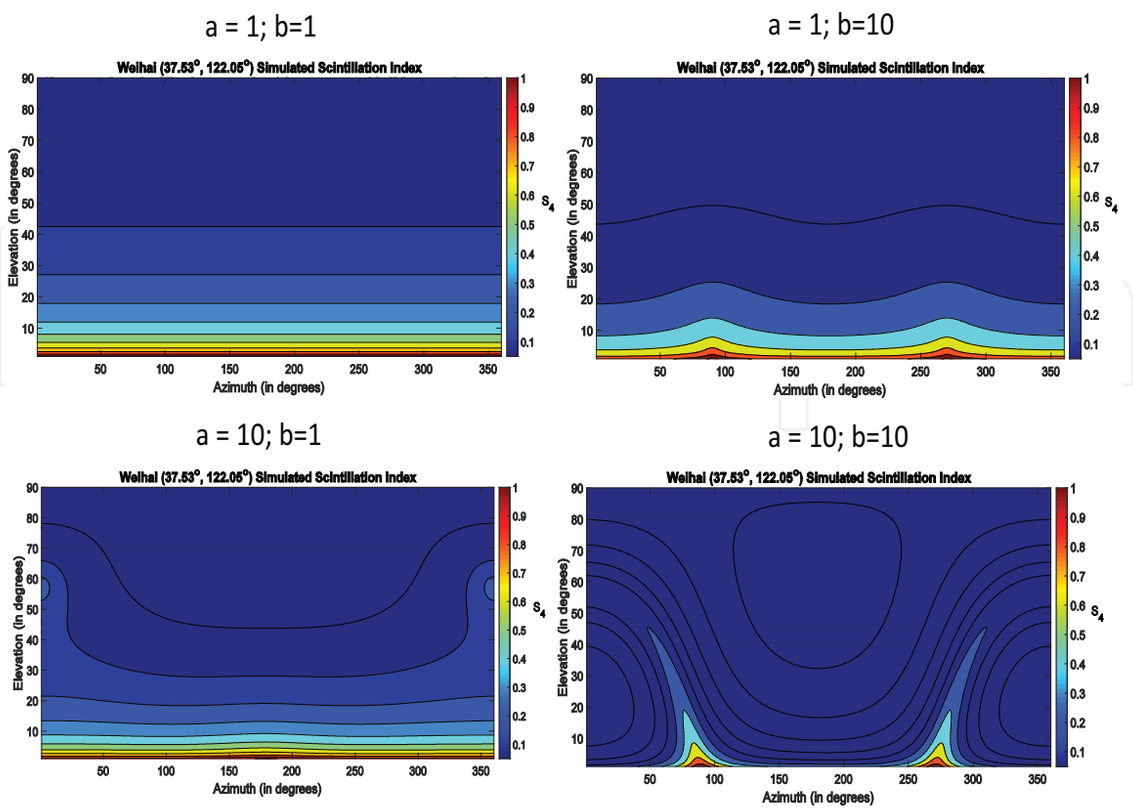

Figure 3.
Simulation scintillation indices for the different combinations of the ionospheric irregularity elongation parameters: rodlike (top-left), winglike (top-right and bottom-left), and sheetlike (bottom-right).

nor across the geomagnetic field lines, then the strength of the scintillation solely depends on the elevation angles. When the spread of the ionospheric structures are more either along (bottom-left) or across (top-right) the geomagnetic field lines, then the numerical value of the scintillation index depends on the combination of the elevation angle and azimuth and on the orientation of the irregularities with respect to the local geomagnetic field lines. As we can see that even for the winglike structures, the scintillation behavior is different for the irregularity spread along and across the geomagnetic field lines. For a = 1 and b = 10 (top-right figure), it shows the decrease in the scintillation with increasing elevation angle, and it also shows scintillation maximizes near two azimuth angles nearly 90° and 270°, respectively. At these two azimuth angles, the line of sight of the observer goes close to the vertical direction of the geomagnetic field lines; ionospheric irregularity structure orientations are vertical and in the direction of the geomagnetic field line. Due to such vertical irregularity orientation, we observe the sharp enhancement in the scintillation index. The third case (a = 10 and b = 1; bottom-left) seems quite similar to the case discussed in the figure at the top-left (a = 1 and b = 1), except 300° > azimuth<50°. In the fourth case (a = 10 and b = 10; bottom-right), there are two spikes at the azimuth 90° and 270°; these spikes are due to the direction of the geomagnetic field effect as well as a gradual decrease in the scintillation with increasing elevation angle. In summary, a certain combination of azimuth and elevation angle and orientation of the geomagnetic field allow radio-wave satellite signal passing more through the ionospheric irregularity structure.

3.2 Limitations as well as efficacy in modeling the scintillation, due to solar activity, local seasons, local time, and geomagnetic activity

It is very challenging to model ionospheric scintillation during different solar activity, season, local time, and geomagnetic activity conditions. The first limitation for empirical modeling may be due to the specific data unavailability during the particular geomagnetic, solar, and local seasons/time conditions. The modeler should be very careful in making the scintillation model sensitive to the several ionospheric anomalies that appear at different geographic locations and seasons. For example, winter anomaly causes more ionospheric scintillation production during the winter months than the summer months in mid-latitude regions. ±20° of the magnetic equator is the equatorial anomaly region. In the equatorial anomaly region, we observe strong ionospheric scintillation as a lot of scintillation-producing ionospheric irregularity deposit in these regions due to the fountain effect. At the equatorial electrojet regions which are at ±3° of the magnetic equator, we also observe severe ionospheric scintillations. Other events such as X-rays, sudden ionospheric disturbances (SID); protons, polar cap absorption (PCA); and geomagnetic storms and lightning can also produce a significant amount of scintillation-producing ionospheric irregularities.

On the other hand, at the polar latitudes, it is widely believed that the phase scintillation index is more sensitive to the solar/geomagnetic events than the amplitude scintillation index [14–17]. Let us understand this by an illustrative example. Following the South Pole scintillation model developed by Priyadarshi et al. [18], we have produced modeled amplitude and phase scintillation maps for two geomagnetic storms, which occurred in the year 2014 (please see **Figures 4** and **5**). This South Pole empirical scintillation model uses two b-spline functions of degree 4, along with the Ap index and scintillation observation recorded over South Pole GSV4004 scintillation receiver (location, 89.99° geographic latitude; 93.77° geographic longitude; geomagnetic coordinate, 73.5°, 127.8°). Since the model uses a single GPS receiver data, therefore, MLT time lags by 4 hours and 22 minutes to the

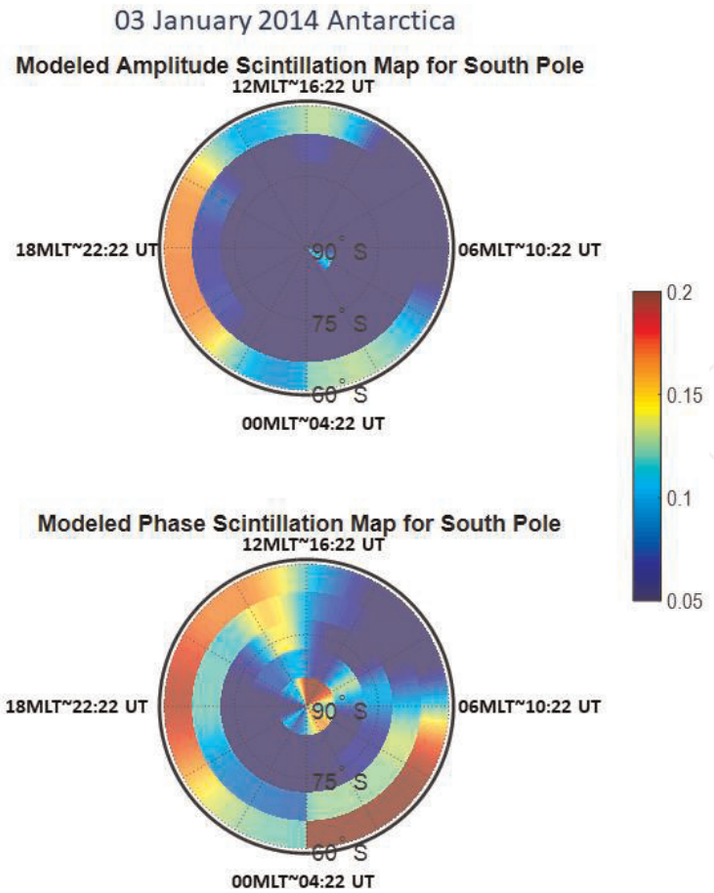

Figure 4.
Modeled amplitude and phase scintillation index over Antarctica during a moderate geomagnetic storm that occurred on 03 January 2014.

universal time hours (UT). As evident from **Figure 4** (between 60 and 70° MLAT), during a weak geomagnetic storm (−30 > =Dst > = −50 nT) that occurred on 03 January 2014, the amplitude scintillation index shows quite similar fluctuations with the phase scintillation index (please see 16–20 MLT at 60–70° S CGMLAT; 0–6 MLT at 60–70° S CGMLAT, and 10–14 MLT at 60–70° S CGMLAT). But, overall phase scintillation values were relatively higher than the amplitude scintillation index. However, during a strong geomagnetic storm (Dst < = − 100 nT) that occurred on 27 February 2014, we see that some part of the amplitude scintillation index shows resemblance with the phase scintillation index map, for instance, 0–2 MLT and 16–18 MLT at 60–70° CGMLAT, but, in the rest of the part near the dusk regions at all the CGMLATs 60–90° S CGMLAT, phase scintillation indices are much higher and high in occurrence than the amplitude scintillation index. It should be noted here that it is not compulsory that S_4 and σ_φ have similar character of variations. In general it depends on the scale of the ionospheric turbulences. In case of kilometers size, the refractive scintillations of the phase are predominant, but amplitude scintillations are minimal. In case of hundred meter-sized turbulence, both refractive and diffractive mechanisms are present, and, hence S_4 and σ_φ indices have high similarity of variations (please see [19] for details).

Space physicist generally explains this that during such strong geomagnetic storms, large-scale ionospheric irregularity structures often enter from the cusp region, and following the convection cells, they pass through the deep inside the polar cap and exit near the magnetic midnight or dusk sector of the polar region. This explanation seems true, but, following the scintillation theory described in Wernik et al. [1], when phase scintillation index keeps on increasing but amplitude

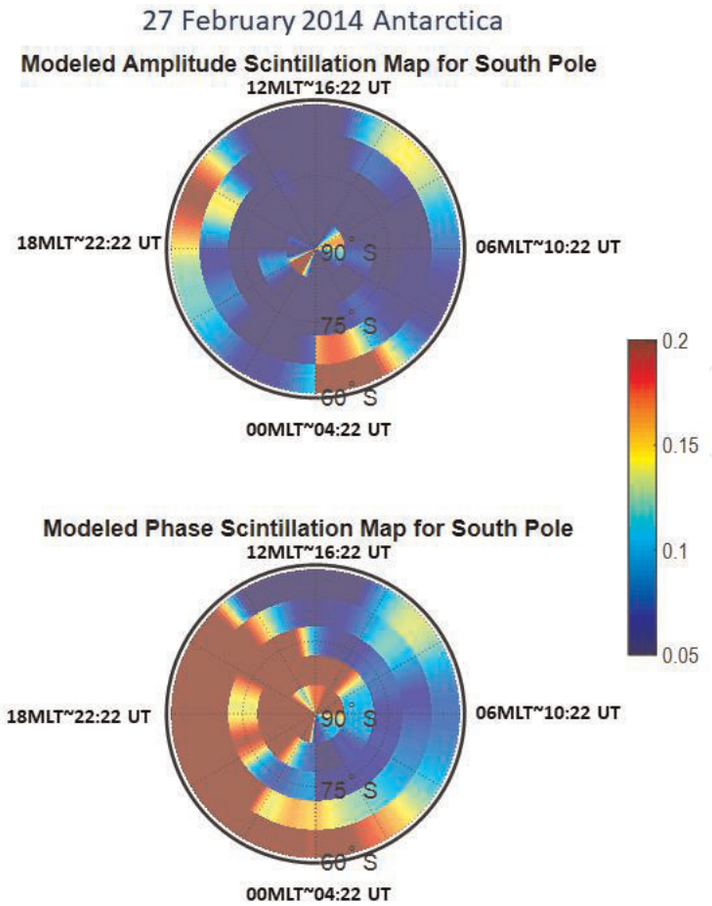

Figure 5.
Modeled amplitude and phase scintillation index over Antarctica during a strong geomagnetic storm that occurred on 27 February 2014.

scintillation seizes to increase, then at this instance, the ionospheric irregularity plasma waves are not more coherent, and these fluctuations cannot be considered as real scintillation due to lack of interference between two noncoherent plasma waves at high-phase fluctuations [1]. For this situation the modeler must optimize the numerical scales of the observed scintillation indices such that the amplitude and phase scintillation indices show similar fluctuation to each other. Priyadarshi et al. [20] used an optimized numerical scale for the amplitude and phase scintillation indices observed during a geomagnetic storm that occurred on 27 February 2014. Ionospheric scintillation index optimization is a way in which by using different amplitude and phase scintillation variation scale it helps us see the same trend variation in the amplitude/phase scintillation indices. In the event discussed in Priyadarshi et al. [20], phase scintillation index variations were optimized between 0.05 and 0.5, and amplitude scintillation index variations were optimized between 0.05 and 0.2. The dayside cusp region amplitude and phase scintillation indices gave similar information at different numerical scales. This study also demonstrated that the amplitude scintillation index is also a useful scintillation index if the proper numerical scale is chosen. Large-scale ionospheric irregularities such as storm-enhanced density (SED) and tong of ionization (TOI) were not found necessarily producing ionospheric scintillation [20].

4. Summary

In general it is more typical when the carrier-phase loss of lock happens due to the sharp signal-to-noise ratio fading (please look [21, 22] for more details). In this book chapter, we have discussed some peculiar modeling tricks and tips of

ionospheric scintillation. If taken care well, the model limitations caused due to geometrical effects such as multipath, elevation angle dependence, and form of ionospheric irregularities can be reduced, and the modeled results would provide an error-free estimation of the scintillation indices. Scintillation observations are one of the scintillation model input. By studying the log-log variation of the scintillation index, we can derive the scintillation index correction parameters as discussed in Section 2 [13]. These scintillation correction parameters are used to correct the scintillation model input data. We have demonstrated the geometric corrections between the satellite and receivers (see **Figure 1**) and its importance to use corrected scintillation indices as model input for modeling the ionospheric scintillation indices. Ionospheric scintillation highly depends on the orientation as well as the spread of the ionospheric irregularities with respect to the local geomagnetic field lines. In order to get the real and justified model's output, we must use the input scintillation data in our model for all available, local seasons, local time, and solar/geomagnetic activity duration. At certain elevation angles, scintillation indices show unusual enhancement (please see **Figure 2**); it is because the signal travels long distances through the ionospheric irregularity structures at the lower elevation angle, and at certain elevation angle, the receiver look along the vertical orientation of the ionospheric irregularities with respect to the local geomagnetic field line. The orientation of the ionospheric irregularities structures influences the ionospheric scintillation intensity. We have compared the four types of combination of ionospheric irregularity structures using four different combinations of elongation axial ratios "a" and "b" (please see **Figure 3** and its related discussion). **Figure 3** demonstrated that at a few combinations of azimuth and elevation angles, the orientation of the geomagnetic field allows radio-wave satellite signal passing more through the ionospheric irregularity structure. Apparently, scintillation intensity enhances at these locations. Through two modeled South Pole scintillation maps during the moderate and strong geomagnetic storms (case studies related to **Figures 4** and **5**), we have demonstrated that the adoption of the scintillation model provides its high case sensitive to the latitudinal anomalies. For example, winter anomaly which occurs at the mid-latitude ionosphere that causes more scintillation occurrence in winter months as compared to the summer months enhanced scintillation $\pm 20°$ to either side of the geomagnetic equator and EEJ effect which occurs $\pm 3°$ on either side of the geomagnetic equator. For high-latitude scintillation modeling, it is essential to consider the ionospheric ionization difference during the sunlit months and dark months. The importance of optimizing the numerical scale of phase and amplitude scintillation indices at the polar latitudes is also discussed. In summary, the presented book chapter discusses all the factors that significantly influence the ionospheric scintillation and possible methods to minimize the estimation errors that caused them. Physics-based models are good to produce the global morphology of the ionospheric scintillation, but, they often fail to produce the exact scintillation index during active solar events. Therefore, empirical models are better as they use the physics-based model as background, but they keep on using the real observations as the model input. These joint efforts work in the derivation and development of a decent ionospheric scintillation model, which can produce equivalent scintillation indices for all the geographic latitudes, local weather, local time, and solar/geomagnetic activity conditions.

Acknowledgements

The scintillation data used in this book chapter has been thankfully obtained from the Polish Polar Station Hornsund, Svalbard. We also thank the Space Research Centre, Polish Academy of Sciences (SRC-PAS) for requesting this data.

Conflict of interest

S. Priyadarshi is the principal as well as the corresponding author of this book chapter. The text, as well as figures presented in this book chapter, has not been published anywhere else before.

Author details

Shishir Priyadarshi
Department of Climatology and Atmospheric Protection, University of Wroclaw, Poland

*Address all correspondence to: shishir.priyadarshi@uwr.edu.pl

References

[1] Wernik AW, Alfonsi L, Materassi M. Ionospheric irregularities, scintillation and its effect on systems. Acta Geologica Polonica. 2004;**52**(2):237-249

[2] Wernik AW, Alfonsi L, Materassi M. Scintillation modeling using in situ data. Radio Science. 2007;**42**:RS1002. DOI: 10.1029/2006RS003512

[3] Singleton DG. Dependence of satellite scintillations on zenith angle and azimuth. Journal of Atmospheric and Terrestrial Physics. 1970;**32**(5): 789-803. DOI: 10.1016/0021-9169 (70) 90029-2

[4] Briggs BH, Parkin IA. On the variation of radio star and satellite scintillations with zenith angle. Journal of Atmospheric and Terrestrial Physics. 1963;**25**(6):339-366. DOI: 10.1016/0021-9169(63)90150-8

[5] Forte B, Radicella SM. Comparison of ionospheric scintillation models with experimental data for satellite navigation applications. Annales de Geophysique. 2005;**48**(3):505-514

[6] Current IGS Site Guidelines. Available from: https://kb.igs.org/hc/en-us/articles/202011433-Current-IGS-Site-Guidelines

[7] Padma B, Kai B. Performance analysis of dual-frequency receiver using combinations of GPS L1, L5, and L2 civil signals. Journal of Geodesy. 2019;**93**:437-447. DOI: 10.1007/s00190-018-1172-9

[8] McCaffrey AM, Jayachandran PT. Spectral characteristics of auroral region scintillation using 100 Hz sampling. GPS Solutions. 2017;**21**:1883-1894. DOI: 10.1007/s10291-017-0664-z

[9] Rino CL. A power law phase screen model for ionospheric scintillation: 1. Weak scatter. Radio Science. 1979; **14**(6):1135-1145. DOI: 10.1029/RS014i006p01135

[10] Ma G, Maruyama T. A super bubble detected by dense GPS network at east Asian longitudes. Geophysical Research Letters. 2006;**33**:L21103

[11] Demyanov VV, Yasyukevich Yu V, Ishin AB, Astafyeva EI. Effects of ionosphere super-bubble on the GPS positioning performance depending on the orientation relative to geomagnetic field. GPS Solutions. 2012;**16**:181-189. DOI: 10.1007/s10291-011-0217-9

[12] Booker HG, Ratcliffe JA, Shinn DH. Diffraction from an irregular screen with applications to ionospheric problems. Philosophical Transactions of the Royal Society. 1950;**242**(856): 579-607. DOI: 10.1098/rsta.1950.0011

[13] Priyadarshi S, Wernik AW. Variation of the ionospheric scintillation index with elevation angle of the transmitter. 2013:**61**(5):1279-1288. DOI: 10.2478/s11600-013-0123-3

[14] Spogli L, Alfonsi L, De Franceschi G, Romano V, Aquino MHO, Dodson A. Climatology of GPS ionospheric scintillations over high and mid latitude European regions. Annales de Geophysique. 2009;**27**(9):3429-3437

[15] Li GZ, Ning BQ, Ren ZP, Hu LH. Statistics of GPS ionospheric scintillation and irregularities over polar regions at solar minimum. GPS Solutions. 2010;**14**(4):331-341

[16] Prikryl P, Jayachandran PT, Mushini SC, Pokhotelov D, Mac-Dougall JW, Donovan E, et al. GPS TEC, scintillation and cycle slips observed at high latitudes during solar minimum. Annales de Geophysique. 2010;**28**(6): 1307-1316

[17] Moen J, Oksavik K, Alfonsi L, Daabakk Y, Romano V, Spogli L. Space weather challenges of the polar cap ionosphere. Journal of Space Weather and Space Climate. 2013;**3**: A02. DOI: 10.1051/swsc/2013025

[18] Priyadarshi S, Zhang QH, Ma YZ, Wang Y, Xing ZY. Observations and modeling of ionospheric scintillations at South Pole during six X-class solar flares in 2013. Journal of Geophysical Research: Space Physics. 2016;**121**: 5737-5751. DOI: 10.1002/2016JA022833

[19] Bhattacharrya A et al. Nighttime equatorial ionosphere: GPS scintillations and differential carrier phase fluctuations. Radio Science. 2000;**35**(1): 209-224

[20] Priyadarshi S, Zhang QH, Ma YZ. Antarctica SED/TOI associated ionospheric scintillation during 27 February 2014 geomagnetic storm. Astrophysics and Space Science. 2018; **363**:262. DOI: 10.1007/s10509-018-3484-x

[21] Tiwari R, Strangeways HJ. Regionally based alarm index to mitigate ionospheric scintillation effects for GNSS receivers. Space Weather. 2015;**13**:72-85. DOI: 10.1002/2014SW001115

[22] Kinter PM, Ledvina BM, de Paula ER. GPS and ionosphere scintillations. Space Weather. 2007; **5**:S09003. DOI: 10.1029/2006SW000260